# Surface Emissivity Retrieved with Satellite Ultraspectral IR Measurements for Monitoring Global Change

Daniel K. Zhou*[1], Allen M. Larar[1], Xu Liu[1], William L. Smith[2,3], and Peter Schlüssel[4]

[1]NASA Langley Research Center, Hampton, VA, USA
[2]Hampton University, Hampton, VA, USA
[3]University of Wisconsin-Madison, Madison, WI, USA
[4]EUMETSAT, Darmstadt, Germany

## ABSTRACT

Surface and atmospheric thermodynamic parameters retrieved with advanced ultraspectral remote sensors aboard Earth observing satellites are critical to general atmospheric and Earth science research, climate monitoring, and weather prediction. Ultraspectral resolution infrared radiance obtained from nadir observations provide atmospheric, surface, and cloud information. Presented here is the global surface IR emissivity retrieved from Infrared Atmospheric Sounding Interferometer (IASI) measurements under "clear-sky" conditions. Fast radiative transfer models, applied to the cloud-free (or clouded) atmosphere, are used for atmospheric profile and surface parameter (or cloud parameter) retrieval. The inversion scheme, dealing with cloudy as well as cloud-free radiances observed with ultraspectral infrared sounders, has been developed to simultaneously retrieve atmospheric thermodynamic and surface (or cloud microphysical) parameters. Rapidly produced surface emissivity is initially evaluated through quality control checks on the retrievals of other impacted atmospheric and surface parameters. Surface emissivity and surface skin temperature from the current and future operational satellites can and will reveal critical information on the Earth's ecosystem and land surface type properties, which can be utilized as part of long-term monitoring for the Earth's environment and global climate change.

**Keywords:** Remote sensing, ultraspectral instrument, inversion, surface emissivity, global change.

## 1. INTRODUCTION

Surface emissivity and surface skin temperature from the current and future operational satellites can and will reveal critical information on the Earth's ecosystem and land surface type properties. The Earth Observing System (EOS) Aqua satellite with the Atmospheric InfraRed Sounder (AIRS) on board was launched on 4 May 2002. Satellite ultraspectral data (such as from AIRS) has been shown to be significant to atmospheric research and monitoring the Earth's environment[1]. The Infrared Atmospheric Sounding Interferometer (IASI)[2], on the Metop-A satellite[3], launched on 19 October 2006, is the first of the advanced ultra-spectral resolution temperature, humidity, and trace gas sounding instruments being flown as part of the Initial Joint Polar System (IJPS) of POES (U.S. Polar Orbiting Environmental Satellites) and EPS (EUMETAT Polar System) programs, the precursor of the Joint Polar System (JPS) of National Polar-orbiting Operational Environmental Satellite System (NPOESS) and EPS operational satellites for the purpose of improved weather, climate, and air quality observation and forecasting. Future satellite systems, such as the IASI on the European Metop-B and -C satellites and the Cross-track Infrared Sounder (CrIS) on the NPOESS Preparatory Project and the continuing series of NPOESS satellites, will continue to provide ultraspectral IR radiance observations that will be used for long-term monitoring for the Earth's environment and global climate change. Long-term and large-scale observations needed for global change monitoring and other research can only be supplied by remote sensing[4]. Surface emissivity retrieved from satellite ultraspectral IR measurements can be greatly beneficial but not limit the assimilation of hyperspectral resolution IR radiances in numerical weather prediction models, the climate simulation, and the surface temperature retrieval from other satellite broad-band measurements. In this paper, a retrieval algorithm is briefly

*daniel.k.zhou@nasa.gov, Tel: +1 757-864-5663

described with samples demonstrating surface emissivity spectra retrieved from different surface types. Global surface emissivity with a spatial resolution of 0.5×0.5 degrees of latitude-longitude are produced with temporal variation to indicate seasonal diversity of global land surface emissivity. We demonstrate the emissivities rapidly retrieved with IASI satellite global measurements in conjunction with some initial retrieval analyses. IASI is a Michelson interferometer with spectral coverage between 3.6 and 15.5 μm. At nadir, the instrument samples data at intervals of 25 km along and a cross track, each sample having a maximum diameter of about 12 km. We are to demonstrate that surface emissivity from satellite measurements can be used in assistance of monitoring global change.

## 2. RETRIEVAL ALGORITHMS AND PERFORMANCE ANALYSIS

The retrieval algorithm described herein only uses IR ultraspectral data; no other data from satellite or surface-based instruments nor from numerical weather analysis/prediction models is utilized in assisting or constraining the retrieval products. The emissivity retrieval algorithm was initially developed with the NPOESS Airborne Sounder Testbed Interferometer (NAST-I)[5] to retrieve emissivity EOF (empirical orthogonal function) coefficients using regression retrieval[6,7]. The concept of retrieving emissivity EOF coefficients was later applied to the AIRS data with EOF regression[8,9], followed by a physical retrieval[10,11]. Global emissivity retrieval has been demonstrated previously by AIRS data. As the regression retrieval is at least 50 times faster than channel based physical retrieval; it is worthwhile to re-evaluate emissivity retrievals to understand whether or not their accuracy is satisfactory in accurately producing other impacted geophysical parameters.

The IASI fast transmittance model used herein is a combination of the Stand-alone AIRS Radiative Transfer Algorithm (SARTA)[12] Version 1.07 and the physically-based cloud radiative transfer model based on the DIScrete Ordinate Radiative Transfer (DISORT)[13] calculations performed for a wide variety of cloud microphysical properties[14]. The retrieval algorithm used for IASI is based on that first developed and demonstrated with NAST-I using an EOF regression-training database that consists of 15,150 profiles obtained from the SeeBor database[15]. The surface emissivity spectrum used with each training profile is randomly selected from a set of laboratory measured emissivity spectra for a wide variety of surface types[16]. The cloud microphysical properties are also simulated. A random number generator is used to specify cloud visible optical depth equally distributed within a pre-specified range. A parameterization based on the balloon and aircraft cloud microphysical database[17] is used to specify cloud effective particle diameter ($D_e$) from the cloud optical depth ($\tau_{cld}$). An iterative one-dimensional variational (1-d var.) multi-variable inversion using the minimum-information regularization method[18] is used for obtaining the final retrieval in this system with emissivity obtained from the regression retrieval. An all-season global EOF regression database is used to obtain the initial profile for the 1-d var. physical retrieval. The physical iterative retrieval can effectively, but not fully, account for non-linearity and further improves retrieval accuracy from the initial profile produced by EOF linear regression. The regression coefficients are still classified with respect to cloud-free and cloudy conditions. The algorithm and other details are found elsewhere[18,19]. The weighting functions (i.e., Jacobians) can be calculated by an analytical scheme or a numerical perturbation method. The channels in these spectral regions can be used for temperature and water vapor profile retrieval[6,18]. Detailed IASI retrieval algorithms including both regression and physical retrieval with case validation have been published recently elsewhere[20].

The emissivity is produced by the regression retrieval only and the rest of the retrieved parameters are further improved with a 1-d var. physical retrieval. Minimal cross talks between parameters to be retrieved are inevitable even in physical retrieval (e.g., between the emissivity and the skin temperature as well as boundary layer temperature/moisture). Since the emissivity is nearly linear, we chose to use retrieved emissivity from linear EOF regression, not further retrieved in physical iteration, in order to reduce the number of variables in the physical retrieval and to effectively finalize other non-linear parameters. Based on our retrieval analyses over IASI global measurements, an improved regression algorithm has been introduced. Several major modifications made to our previous algorithm are listed herein. It is noted that some of them are made from our empirical experiences through retrieval simulation analyses and real data retrieval validations. It involves more channels in the window regions, however the shortwave channels beyond 2220 $cm^{-1}$ are not used to avoid solar effect that currently cannot be modeled accurately, especially for occasional sun-gleams into the sensor. The solar zenith angle is included in the training and retrieval process to take care of the solar radiation which still has small but significant impact on the selected channel radiances for emissivity retrieval. Figure 1 shows the retrieval channels currently used for regression and physical retrieval.

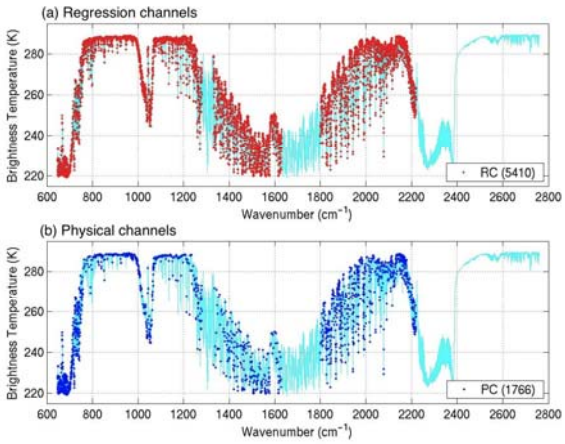


Fig. 1. Retrieval channels indicated over IASI spectrum: (a) 5410 channels used in the regression retrieval (i.e., regression channel: RC); (b) 1766 channels used in the physical retrieval (i.e., physical channel: PC).

Retrieval analysis has been performed to assess the retrieval accuracy including surface parameters using SeeBor database for a dependent simulation. Land surface parameters' retrieval accuracies are improved with a more diverse contrast of surface skin and air temperature, especially over extreme hot and/or cold (e.g., desert and/or polar) regions. Land surface skin temperature in the SeeBor training database has been modified by

$$T_s' = T_a + (T_s - T_a) \times 1.8, \tag{1}$$

where $T_a$ and $T_s$ are surface air and skin temperature, respectively.

A surface emissivity function is used instead of emissivity in the retrieval in order to constrain retrieved emissivity spectrum ($\varepsilon_\nu$) within a boundary between $\varepsilon^{\min}$ and $\varepsilon^{\max}$. We introduce an emissivity function

$$F(\varepsilon_\nu) = \log[\log(\varepsilon^{\min}) - \log(\varepsilon^{\max} - \varepsilon_\nu)] \tag{2}$$

to be used in the training and retrieval algorithm. The $\varepsilon^{\min}$ (i.e., 0.5) and $\varepsilon^{\max}$ (i.e., 0.995) are preset to the best of our knowledge for surface emissivities. Eigenvectors of $F(\varepsilon_\nu)$ and associated amplitudes are generated and used in the regression equation. The emissivity is computed later from the emissivity function $F(\varepsilon_\nu)$ that is calculated from retrieved 10 EOF amplitudes of $F(\varepsilon_\nu)$. It is worth mentioning that the emissivity is retrieved rapidly since the cloud detection and emissivity retrieval are done within the same EOF regression; the data volume is small since the emissivity is compressed in the EOF domain.

Cloud detection criteria in the regression are re-investigated in order to provide accurate "cloud-free" single field-of-view (SFOV) measurements. Multi-stage regression retrievals are performed. The first-stage involves mixed (i.e., clear and cloudy) regression. The second-stage (e.g., either clear or cloudy) depends on the cloud detection criteria that are based on first-stage retrieved cloud parameters (i.e., $H_c$ is cloud top height relative to surface, $\phi$ is cloud phase, and $\tau_{cld}$ is cloud visible optical depth). The second-stage will use clear regression coefficients when the first retrieval satisfies these criteria

1. $H_c \le 2.5$ km, and
2. $\phi \le 0.5$, and
3. $\tau_{cld} \le 0.005$,

where $\phi = 0$, 1, and 2 are for clear conditions, ice cloud, and water clouds, respectively. Otherwise, the second-stage will use cloudy regression coefficients. When the second-stage is using cloudy regression, an additional clear regression will be performed if one of three following criteria is met from the second-stage cloudy retrieval,

1. $\tau_{cld} \le 0.1$,
2. $H_c \le 2.0$ km and $\tau_{cld} \le 0.2$, and
3. $H_c \le 2.5$ km and $\tau_{cld} \le 0.3$.

Actually, it should be explained that so called "clear-sky" cases from this analysis are "cloud undetected." They can be either real clear or contain a minimal cloud fraction almost not interfering with the retrieval.

Surface emissivity ($\varepsilon$) is often used as a constant ($\varepsilon \approx 1$), especially over the water, in the retrieval process for satellite measurements due to lack of emissivity knowledge. However, the emissivity is a function of wavelength (or wavenumber) and it deviates significantly from one over the land, especially over a desert or barren surface. Research on the emissivity (or reflectivity) and measurements over different types of material samples commonly existing over the Earth's surface have been conducted[16]. Satellite measurements concur that surface emissivity contributes significantly to the total transmittance measured by the satellite instruments. Samples shown in Figure 2 are for both day and night observations over the Sahara Desert. Simulated spectral radiances from the retrieved parameters (i.e., atmospheric profiles, surface skin temperature and emissivity) are plotted in Figures 2a and 2c (red curves) in comparison with the measurements (blue curves). Retrieved surface emissivity spectra are plotted in Figures 2b and 2d with IASI day and night observations, respectively. If retrieved emissivity is replaced with a unity emissivity, the simulated spectra (green curves) in the window regions significantly deviate from the measurements. This indicates that surface emissivity information is evident in the observations and it has to be taken into an account in order to accurately retrieve other surface and atmospheric parameters.

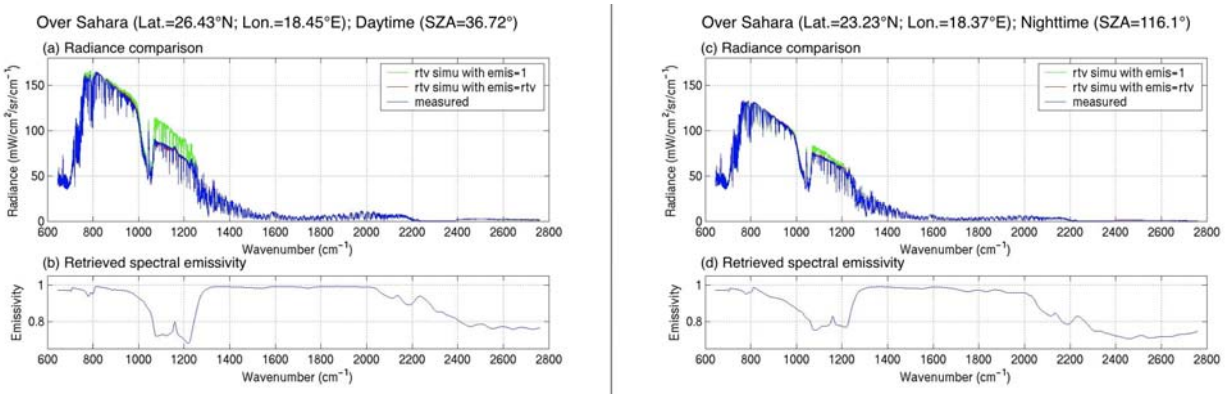


Fig. 2. Samples of surface emissivity retrieved over Sahara Desert from both day and night. Radiance simulations with retrievals are compared with the measurements (see text).

It is worth mentioning that, in the radiative transfer equation under clear-sky conditions, channel radiance $I_\nu$ at a certain wavenumber is computed by

$$I_\nu = \int_0^z B_\nu[T(z)] \cdot \frac{\partial \tau_\nu(z,\, z^s)}{\partial z} \cdot dz + \rho_\nu \cdot \tau_\nu(0,\, z^s) \cdot \int_\infty^0 B_\nu[T(z)] \frac{\partial \tau_\nu(z,\, z^s)}{\partial z} \cdot dz + \varepsilon_\nu \cdot B_\nu(T_s) \cdot \tau_\nu(0,\, z^s) + \rho_\nu^{solar} \cdot H \cdot \tau_\nu^b(0,\, z^s,\, \theta) \cdot \cos(\theta)\,, \tag{3}$$

where $I_\nu$, $\varepsilon_\nu$, $B_\nu$, $T_s$, $\tau_\nu(z_1, z_2)$, $z^s$, $T(z)$, $\rho_\nu$, $\rho_\nu^{solar}$, $H$, $\theta$, $\tau_\nu^b$ are observed spectral radiance, spectral emissivity, spectral Planck function, the surface temperature, spectral transmittance from altitude $z_1$ to $z_2$, sensor altitude, spectral surface reflectivity, spectral solar reflectivity, solar irradiance, solar zenith angle, and two-path transmittance from the Sun to the surface to the satellite respectively. Here, diffused reflection is assumed; the spectral solar reflectivity and the

spectral surface IR thermal reflectivity are assumed to be a function of surface emissivity, such as $\rho_v^{solar} = (1-\varepsilon_v)/\pi$ and $\rho_v = (1-\varepsilon_v)$, respectively. Because of the lack of these parameters, the above assumptions are used based on the best of our knowledge. However, they are not realistic and introduce emissivity retrieval errors, especially during the daytime, while additional solar radiation needs to be taken into an account. These retrieval errors, including "ill-posed" retrieval uncertainties of atmospheric thermodynamics parameters, are indicated in the simulated radiances as shown in Figure 2 (i.e., the difference between measured and retrieval simulated spectra).

Retrieval accuracy can be estimated by taking advantage of radiative transfer model simulation in obtaining synthetic observed radiances. The truth profile (i.e., the radiosonde observation) is known and the retrieval can be directly compared with the truth to define retrieval accuracy due to (1) instrumental noise, and (2) retrieval error introduced by the so-called "ill-posed" retrieval model. The disadvantage of this approach is that errors in the forward radiative transfer model are not included (e.g., the correlation assumed between emissivity and reflectivity). However, detailed validation in estimating both forward and inversion model errors can be fulfilled with dedicated field campaigns. Atmospheric conditions are coincidently captured by multi-instruments from both ground and aircraft validation sites[9,21], where dedicated coincident radiosondes were launched under satellite overpasses for a reasonable period of time[22,23]. This atmospheric profile retrieval is a solution of an "ill-posed" problem and its retrieval accuracy is measurement or scene dependent. Thus, it is important to estimate retrieval accuracy through globally synthetic simulations, intensive field campaigns, and validations. The retrieval accuracy analysis with a SFOV retrieval algorithm reported here has been performed through synthetic simulations with IASI instrumental noise over a global dataset for both cloud-free and cloudy conditions. A test dataset is used to simulate IASI observations for physical retrieval performance analysis. It is noted that this kind of error analysis is dependent on the test dataset; however, the analysis can be done over a large set of samples to minimize the bias of the test dataset. Since the absolute retrieval error is observation or scene dependent, retrieval accuracy is represented by the mean difference (i.e., bias) and the standard deviation of the error (i.e., STDE) over a global dataset. The key thermodynamic parameters, such as atmospheric temperature profile, moisture profile, surface skin temperature and emissivity (for cloud-free cases) or cloud microphysical parameters (for cloudy cases), are used to indicate retrieval accuracy over a global dataset. Detail analysis outcomes have been reported on retrieval accuracy for both clear and cloudy conditions[20].

The emissivity assigned to each training profile is randomly selected from a laboratory measured emissivity database, indicated in Figure 3a, and has a wide variety of surface types suitable for different geographical locations. The vertical bars show the emissivity STD for this dataset. The emissivity assigned to the training data is not realistic as the effective surface emissivity is to be retrieved from the satellite measurement, however the training data are what we hoped to cover the combination of the Earth surface emissivity. It is noted that the outcomes from simulation analysis only give us a very rough estimation. Estimated surface emissivity retrieval accuracy, the mean difference (or bias) in curve and the STDE in vertical bars shown in Figure 3b, is training data dependent. In other words, we should evaluate the emissivity accuracy accordingly in conjunction with the emissivity training variability in the emissivity sensitive regions (i.e., window regions). Emissivity is retrieved in conjunction with skin temperature, and atmospheric profiles of temperature and moisture. Since the skin temperature is one of the most "coupled" parameters with emissivity, it is necessary to mention that skin temperature retrieval accuracy has a -0.07°K bias with a 0.84°K STDE from the same analysis. It should be mentioned that the shortwave region has a relatively poor accuracy, which is due to a higher noise level and fewer window channels than that in the longwave region; also the retrieval accuracy is not reliable in the opaque regions as hardly any surface information is contained there.

## 3. GLOBAL LAND SURFACE EMISSIVITY

Global land surface emissivities are retrieved from IASI measurements. The retrievals, limited to IASI FOV, are effective surface emissivities due to non-homogeneous scenes. In other words, the effective surface emissivity can be a combination of all possible materials within the FOV. Due to cloud coverage, not every measurement can provide surface parameters; however, the surface parameters can be retrieved under optically thin clouds but with relatively poor accuracy in comparison with that retrieved under clear-sky conditions[18]. The composition of the surface emissivity can be assembled over a period of time and area. A set of retrievals is used to generate a convoluted surface emissivity. Single retrievals within a spatial grid (area) meeting the following criteria will be taken to generate a convoluted emissivity. These criteria are

1. $\tau_{cld} < 0.5$, and
2. $(\overline{T_s} - \sigma_t) < T_s < (\overline{T_s} + \sigma_t)$, and
3. $(\overline{A_{F1}} - \sigma_{F1}) < A_{F1} < (\overline{A_{F1}} + \sigma_{F1})$, and
4. $N > 4$,

where $\overline{T_s}$, $\sigma_t$, $A_{F1}$, $\overline{A_{F1}}$, $\sigma_{F1}$, and $N$ are $T_s$ mean, $T_s$ STD, first EOF amplitude of $F(\varepsilon)$, $A_{F1}$ mean, $A_{F1}$ STD, and the number of SFOV measurements satisfying criteria 1-3, respectively.

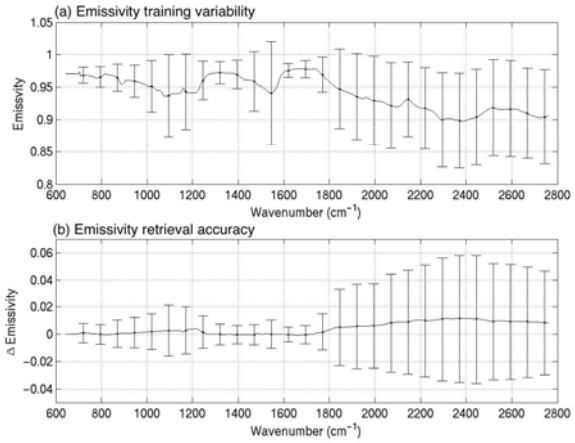


Fig. 3. (a) The mean surface emissivity spectrum for a set of laboratory measured emissivity spectra for a wide variety of surface types suitable for global geographical location. The vertical bars show the STD of the emissivity for this dataset. (b) Estimated surface emissivity retrieval accuracy through IASI simulation with a global database; the curve is the mean difference and the vertical bars are the STDE of the retrieved emissivity against the truth (see text).

With a spatial resolution of 0.5×0.5 degrees of latitude-longitude, monthly-convoluted land surface skin temperature and emissivity are shown in Figures 4 and 5, respectively. As the emissivity is a function of wavenumber (or wavelength), two selected frequencies at 950 cm$^{-1}$ (or 10.5 μm) and 1250 cm$^{-1}$ (or 8.0 μm) are plotted in Figures 5a and 5b, respectively.

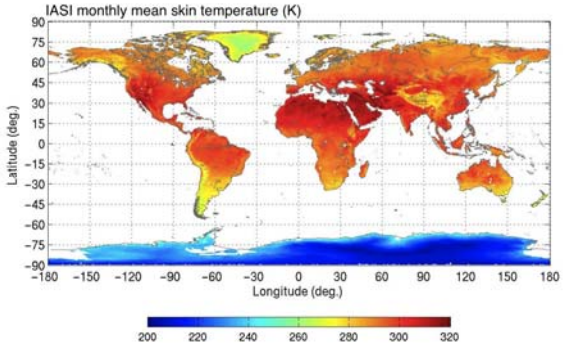


Fig. 4. Monthly-convoluted (July 2007) land surface skin temperature from IASI retrievals. Notice that white areas were covered with clouds.

The surface emissivities reflect the Earth's types and environment including ecosystem health that plays an important role in understanding the impacts of climate changes and human activities on altered degradation, biodiversity, and ecosystem sustainability. Principal deserts, such as Sahara (Northern Africa), Kalahari and Namib (Botswana, South Africa, Namibia, and Angola), Taklamakan and Gobi (China and Mongolia), Great Basin and Mojave (US), Sonoran (US and Mexico), Atacama (Chile), and Patagonian (Argentina), and Australian deserts, are identified on the emissivity map shown in Figure 5. The world's desert can be divided into four categories. Subtropical deserts are the hottest, with parched terrain and rapid evaporation. Although cool coastal deserts are located within the same latitudes as subtropical deserts, the average temperature is much cooler because of frigid offshore ocean currents. Cold winter deserts are marked by stark temperature differences from season to season, ranging from ~311°K (100°F) in the summer to ~261°K (10°F) in the winter[24,25]. Polar regions are also considered to be deserts because nearly all moisture in these areas is locked up in the form of ice. Satellite derived effective land surface emissivity can be used to assist monitoring global change over interested regions such as deserts which generally receive less than ten inches of precipitation a year or the potential evaporation rate is twice as great as the precipitation. Other regions can also be interesting, such as the regions covered by sea ice and glacier.

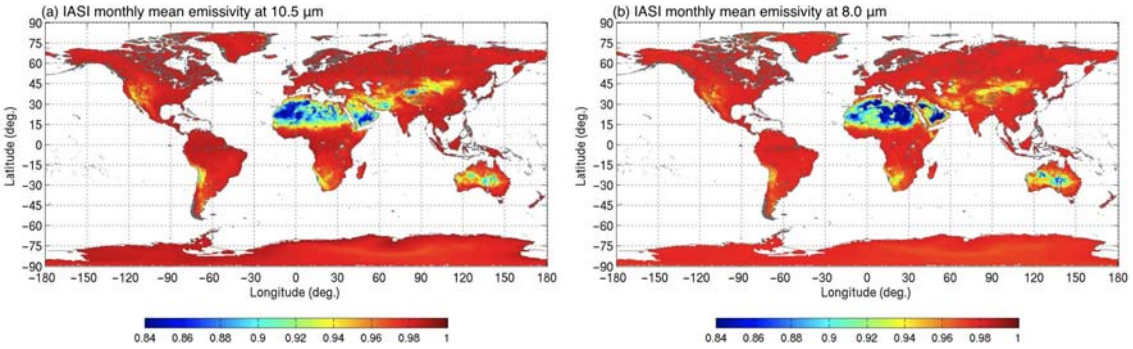


Fig. 5. Monthly-convoluted (July 2007) IASI emissivities at 950 $cm^{-1}$ (10.5 μm) and 1250 $cm^{-1}$ (8.0 μm).

To demonstrate emissivity temporal variation, 2 months worth of data (July and August 2007) are used to produce 10-day convoluted emissivity maps; samples at 10.5 μm and 8.0 μm are shown in Figures 6 and 7, respectively. The American continent is focused on for clarity; the changes of surface emissivity can be seen. These changes, through a 2-month period, are mainly due to seasonal variation and weather conditions (e.g., temperature and rainfall).

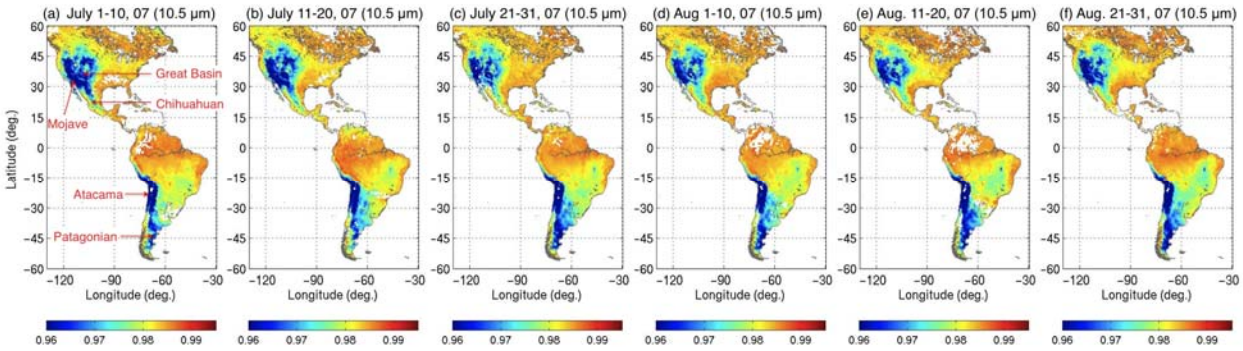


Fig. 6. Temporal variation of 10-day convoluted IASI emissivities at 950 $cm^{-1}$ (10.5 μm). Notice that white areas were covered with clouds.

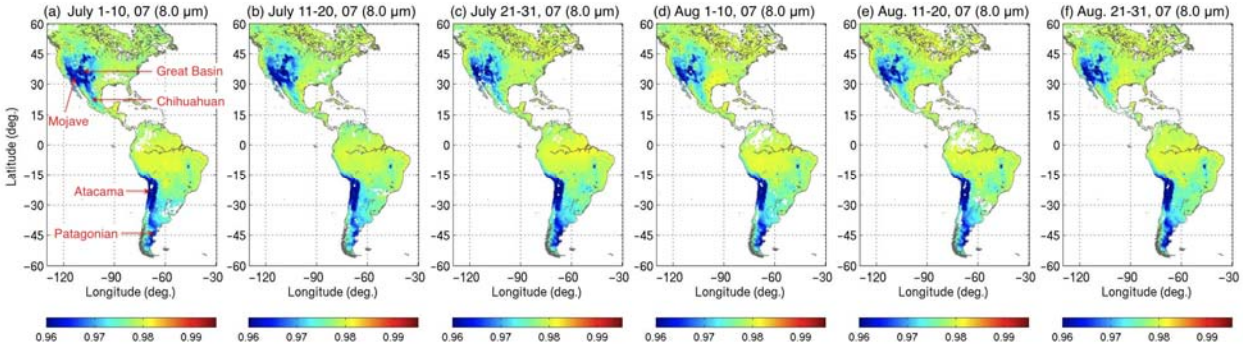


Fig. 7. Same as Figure 6 but at 1250 $cm^{-1}$ (8.0 μm).

Semi-annual variation is also shown in Figure 8 in order to demonstrate the emissivity contrast between summer and winter. The North American continent is focused on for clarity; Figure 8 shows the monthly-convoluted emissivities retrieved from July 2007, January 2008, and their differences between these 2 months at a selected frequency. Relatively speaking, the smaller or larger effective emissivity denotes more or less barren land during the winter or summer. As shown in Figure 8c, a higher or lower emissivity over the Great Basin or the Great Plains is expected because of the snow/ice or barren land (i.e., soil) during the winter season. This implies that global land surface emissivities derived from satellite IR ultraspectral data can be used to capture the change of land surface property, thus having great value in monitoring of the Earth's environment and global change.

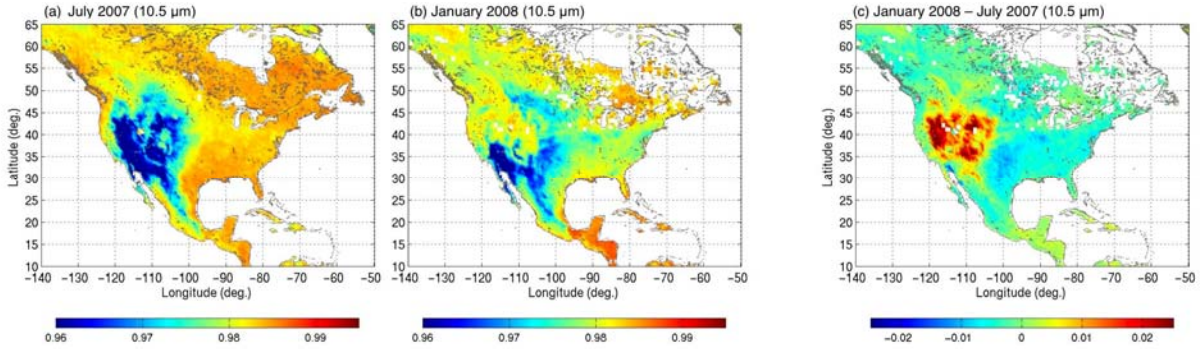


Fig. 8. Semi-annual emissivity variation at 950 $cm^{-1}$ (10.5 μm): (a) and (b) are monthly-convoluted IASI emissivities of July 2007 and January 2008, respectively, and (c) is the emissivity difference between July 2007 and January 2008.

It should be mentioned that the random error of convoluted emissivity over a certain period of time and area is smaller than that from a SFOV (shown in Figure 3). This depends on the number of SFOV emissivity spectra used for one convoluted emissivity spectrum. For example, there could be up to a few hundred SFOV measurements for one month over an area of 0.5×0.5 degrees of latitude-longitude if all these measurements are under "clear-sky" conditions. The convoluted emissivity has its random error reduced by the square root of the number of "clear" measurements, depending on the cloudiness over that period of time and area. However, detailed error estimation needs to be investigated along with validation.

## 4. SUMMARY AND FUTURE WORK

A state-of-the-art retrieval algorithm, dealing with all-weather conditions, has been developed and applied to IASI radiance measurements. Surface emissivity is rapidly retrieved using the multi-stage linear EOF regression. The

seasonal variation of global land surface emissivity derived from satellite IR ultraspectral data is evident. This retrieval process is so fast that it can provide near-real-time result that is desired by the numerical weather prediction (NWP) model analysis using IR hyperspectral simulations[26]. Results from IASI retrievals indicate that surface emissivity is retrieved with satellite IR ultraspectral data to capture different land surface type properties that contain useful information on the terrestrial ecosystem health and reflect on the biosphere's response to proximal climatic factors (such as temperature and rainfall) and human activities. Operational global satellite data, such as that from IASI and CrIS, are and will be available for deriving this kind of product. In conjunction with other satellite products, these can provide information for monitoring the Earth's environment and global change as well as the study of ecosystem health that plays an important role in understanding the impact of climate change and human activity on altered degradation, biodiversity, and ecosystem sustainability. Global land emissivity data compressed in EOF domain can be generated for science community research and other uses. Retrieved emissivity validation will be focused on for providing more-definitive accuracy of the emissivity products. The training database will be improved to include more diverse profiles for cloudy conditions. Criteria for cloud detection will be further enhanced through analysis and validation. Algorithm improvements, along with its product validation, will be made and applied to current and future satellite instruments to provide data for long-term monitoring of the Earth's environment and global change.

## ACKNOWLEDGEMENTS

The authors gratefully acknowledge support from the NASA Langley Research Center and NASA Headquarters. The NAST-I program is supported by NASA Langley Research Center, NASA Headquarters, and the NPOESS Integrated Program Office. IASI has been developed and built under the responsibility of the Centre National d'Etudes Spatiales (CNES). It is flown on-board the Metop satellites as part of the EUMETSAT Polar System. The IASI L1 data are received through the Unified Meteorological Archival and Retrieval Facility (UMARF) of EUMETSAT. The SARTA molecular radiative transfer model and the fast cloud radiative transfer model were provided by Dr. L. L. Strow of the University of Maryland Baltimore County and Dr. P. Yang of Texas A&M University, respectively. The global training database SeeBor was provided by the Space Science and Engineering Center of the University of Wisconsin.

## REFERENCES

[1] Chahine, C., and Coauthors, "AIRS: improving weather forecasting and providing new insights into climate", *B. Am. Meteorol. Soc.*, **87**, 911–926 (2006) [doi:10.1175/BAMS-87-7-911].

[2] Blumstein, D., G. Chalon, T. Carlier, C. Buil, P. Hebert, T. Maciaszek, G. Ponce, and T. Phulpin, "IASI instrument: technical overview and measured performances", *SPIE Proc*. **5543**, 196–207 (2004) [doi:10.1117/12.560907].

[3] Klaes, K. D., M. Cohen, Y. Buhler, P. Schlüssel, R. Munro, J.-P. Luntama, A. Von Engeln, E. Ó. Clerigh, H. Bonekamp, J. Ackermann, J. Schmetz, "An introduction to the EUMETSAT Polar System", *B. Am. Meteorol. Soc.*, **88**, 1085–1096 (2007) [doi:10.1175/BAMS-88-7-1085].

[4] Schädlich, S., F. M. Göttsche, F.-S. Olesen, "Influence of land surface parameters and atmosphere on METEOSAT brightness temperature and generation of land surface temperature maps by temporally and spatially interpolating atmospheric correction," *Remote Sens. Environ*., **75**, 39–46 (2001) [doi:10.1016/S0034-4257(00)00154-1].

[5] Cousins, D., and W. L. Smith, "National Polar-Orbiting Operational Environmental Satellite System (NPOESS) Airborne Sounder Testbed-Interferometer (NAST-I)", *Proc. SPIE*, **3127**, 323–331 (1997) [doi:10.1117/12.279075].

[6] Zhou, D. K., W. L. Smith, J. Li, H. B. Howell, G. W. Cantwell, A. M. Larar, R. O. Knuteson, D. C. Tobin, H. E. Revercomb, and S. A. Mango, "Thermodynamic product retrieval methodology for NAST-I and validation", *App. Opt*., **41**, 6957–6967 (2002) [doi:10.1364/AO.41.006957].

[7] DeSlover, D. H., R. O. Knuteson, B. Osborne, D. K. Zhou, and W. L. Smith, "Validation of aircraft-measured land surface emissivity", *Proc. SPIE*, **4891**, 384–391 (2003) [doi:10.1117/12.466041].

[8] Zhou, D. K., A. L. Larar, W. L. Smith, and X. Liu, "Surface emissivity effects on thermodynamic retrieval of IR spectral radiance", *Proc. SPIE* **6405**, 64051H (2006) [doi:10.1117/12.694283].

[9] Zhou, D. K., W. L. Smith, V. Cuomo, J. P. Taylor, C. D. Barnet, P. Di Girolamo, G. Pappalardo, A. M. Larar, X. Liu, S. M. Newman, C. Lee, and S. A. Mango, "Retrieval validation during the European Aqua Thermodynamic Experiment", *Q. J. R. Meteorol. Soc*. **133**, 203–215 (2007).

[10] Li, J., J. Li, E. Weize, and D. K. Zhou, "Physical retrieval of surface emissivity spectrum from hyperspectral infrared radiances", *Geophys. Res. Lett.*, **34**, L16812 (2007) [doi:10.1029/2007GL030543].
[11] Li, J., and J. Li, "Derivation of global hyperspectral resolution surface emissivity spectra from advanced infrared sounder radiance measurements", *Geophys. Res. Lett*., **35**, L15807 (2008) [doi:10.1029/2008GL034559].
[12] Strow, L. L., S. E. Hannon, S. De Souza-Machado, H. E. Motteler, and D. Tobin, "An overview of the AIRS radiative transfer model", *IEEE Trans. Geosci. Remote Sensing*, **41**, 303–313 (2003) [doi:10.1109/TGRS.2002.808244].
[13] Stamnes, K., S.-C. Tsay, W. Wiscombe, and K. Jayaweera, "Numerically stable algorithm for discrete-ordinate-method radiative transfer in multiple scattering and emitting media", *App. Opt*., **27**, 2502–2509 (1988).
[14] Yang, P., B. C. Gao, B. A. Baum, Y. Hu, W. J. Wiscombe, S.-C. Tsay, D. M. Winker, and S. L. Nasiri, "Radiative Properties of cirrus clouds in the infrared (8-13 μm) spectral region", *J. Quant. Spectros. Radiat. Transfer*, **70**, 473–504 (2001) [doi:10.1016/S0022-4073(01)00024-3].
[15] Seemann, S. W., E. E. Borbas, R. O. Knuteson, G. R. Stephenson, and H.-L. Huang, "Development of a global infrared land surface emissivity database for application to clear-sky sounding retrievals from multi-spectral satellite radiance measurements", *J. Appl. Meteorol. Climatol*., **47**, 108–123 (2008) [doi:10.1175/2007JAMC1590.1].
[16] Salisbury, J. W., and D. M. D'Aria, "Emissivity of terrestrial material in the 8–14 μm atmospheric window", *Remote Sens. Environ.*, **42**, 83–106 (1992) [doi:10.1016/0034-4257(92)90092-X].
[17] Heymsfield, A., J. S. Matrosov, and B. Baum, "Ice water path–optical depth relationships for cirrus and deep stratiform ice cloud layers", *J. Appl. Meteor*., **42**, 1369–1390 (2003) [doi:10.1175/1520-0450(2003)042<1369:IWPDRF>2.0.CO;2].
[18] Zhou, D. K., W. L. Smith, Sr., X. Liu, A. M. Larar, S. A. Mango, and H.-L. Huang, "Physically retrieving cloud and thermodynamic parameters from ultraspectral IR measurements", *J. Atmos. Sci*., **64**, 969–982 (2007) [doi:10.1175/JAS3877.1].
[19] Zhou, D. K., W. L. Smith, X. Liu, A. M. Larar, H.-L. Huang, J. Li, M. J. McGill, and S. A. Mango, "Thermodynamic and cloud parameters retrieval using infrared spectral data", *Geophys. Res. Lett*., **32**, L15805 (2005) [doi:10.1029/2005GL023211].
[20] Zhou, D. K., W. L. Smith, A. M. Larar, X. Liu, J. P. Taylor, P. Schlüssel, L. L. Strow, and S. A. Mango, "All weather IASI single field-of-view retrievals: Case study - Validation with JAIVEx data", *Atmos. Chem. Phys. Discuss*., **8**, 21001–21035 (2008).
[21] Taylor, J. P., and Coauthors, "EAQUATE – An international experiment for hyper-spectral atmospheric sounding validation", *B. Am. Meteorol. Soc.*, **89**, 203–218 (2008) [doi:10.1175/BAMS-89-2-203].
[22] Tobin, D. C., H. E. Revercomb, R. O. Knuteson, B. M. Lesht, L. L. Strow, S. E. Hannon, W. F. Feltz, L. A. Moy, E. J. Fetzer, and T. S. Cress, "Atmospheric Radiation Measurement site atmospheric state best estimates for Atmospheric Infrared Sounder temperature and water retrieval validation", *J. Geophys. Res*., **111**, D09S14 (2006) [doi:10.1029/2005JD006103].
[23] Pougatchev, N., "Validation of Atmospheric Sounders by Correlative Measurements", *App. Opt*., **47**, 4739–4748 (2008) [doi:10.1364/AO.47.004739].
[24] Walton, K., *The Arid Zones*, Transaction Publishers, U.S. (2007).
[25] Weisbrod, N., http://www.waterencyclopedia.com/Da-En/Desert-Hydrology.html
[26] Le Marshall, J., and Coauthors, "Improving global analysis and forecasting with AIRS", *B. Am. Meteorol. Soc.*, **87,** 891–894 (2006) [doi:10.1175/BAMS-87-7-891].